frontiers | Frontiers in Mechanical Engineering

TYPE Original Research
PUBLISHED 19 June 2023
DOI 10.3389/fmech.2023.1204659

OPEN ACCESS

EDITED BY
Jianlin Liu,
China University of Petroleum (East China), Qingdao, China

REVIEWED BY
Han Tang,
Northeast Agricultural University, China
Pei Li,
Xi'an Jiaotong University, China

*CORRESPONDENCE
Lin Chen,
461769837@qq.com

RECEIVED 13 April 2023
ACCEPTED 05 June 2023
PUBLISHED 19 June 2023

CITATION
Wang J, Chen L, Tang Y, Chen Z, Wu Q and Han D (2023), Calibration and experiment of discrete element model parameters of Zanthoxylum bungeanum. *Front. Mech. Eng* 9:1204659.
doi: 10.3389/fmech.2023.1204659

Calibration and experiment of discrete element model parameters of Zanthoxylum bungeanum

Jian Wang, Lin Chen*, Yingwen Tang, Zhifan Chen, Qingsong Wu and Dandan Han

School of Mechanical and Electrical Engineering, Sichuan Agricultural University, Ya'an, Sichuan, China

Zanthoxylum bungeanum is a characteristic spice in culinary culture. This article focuses on the lack of intrinsic and contact parameters for Zanthoxylum bungeanum and studies the intrinsic parameters of the discrete element for tribute pepper from Hanyuan. This is to provide support for the mechanized harvesting of Zanthoxylum bungeanum. The EDEM software was used to establish a discrete element model for Zanthoxylum bungeanum granules. The intrinsic parameters of Zanthoxylum bungeanum granules, such as Three-dimensional dimension, density, Poisson's ratio, and elastic modulus, were measured through experiments. The elastic recovery coefficient, static friction coefficient, and rolling friction coefficient between Zanthoxylum bungeanum granules and Dragon Skin 30 silicone sheets were also measured. Subsequently, the elastic recovery coefficient, static friction coefficient, and rolling friction coefficient between Zanthoxylum bungeanum granules and materials, as well as between Zanthoxylum bungeanum granules were obtained through discrete element simulation experiments, steepest climb test, and Quadratic regression orthogonal rotation combination test. Finally, the Angle of repose was used for verification experiments. The results showed that the elastic recovery coefficient, static friction coefficient, and rolling friction coefficient between Zanthoxylum bungeanum granules and materials were 0.437, 0.758, and 0.0136, respectively, while those between Zanthoxylum bungeanum granules were 0.378, 0.56, and 0.0143, respectively. The error between the simulation angle of repose and the measured angle of repose was 0.204%, verifying the reliability of the discrete element model for Zanthoxylum bungeanum granules. This method is of great significance for the design and optimization of Zanthoxylum bungeanum harvesters.

KEYWORDS

discrete element method, *Zanthoxylum bungeanum* granules, particle modeling, parameter calibration, steepest climb test

1 Introduction

As a local economic plant in China (Lu et al., 2020), Zanthoxylum bungeanum plays an important role for farmers in poor areas to increase their income so as to alleviate their poverty. Zanthoxylum bungeanum picking takes 33%–50% of the labor force which used in the whole production process (Fu, 2011). Picking Zanthoxylum bungeanum is time-consuming and laborious, resulting in high picking costs. In recent years, the planting area of Zan-thoxylum bungeanum has expanded rapidly. By 2021, the planting area of China reached 1.34 million hectares. Nowadays, Zanthoxylum bungeanum harvesting mainly depends on manual harvesting, for which the current shortages include low efficiency, high labor cost, long harvest cycle, etc., seriously hindering the sustainable development of Zanthoxylum bungeanum industry.

In order to make Zanthoxylum bungeanum harvesting more efficient, China has made great efforts on developing agricultural machinery and equipment which are related to Zanthoxylum bungeanum harvesting. For making the picking process more efficient and economic-friendly, Zanthoxylum bungeanum researchers have experimented with high branch picking (Liu et al., 2017), mechanical vibration (Li et al., 2021), negative pressure absorption and other methods. However, due to the characteristics of Zanthoxylum bungeanum, the picking is still inefficient and costly. In recent years, the application of the discrete element method and the simulation software EDEM in the agricultural field has provided a new way for the research on the contact characteristics of agricultural materials and mechanical parts, and has promoted the development of agricultural machinery (Fang et al., 2021; Wang et al., 2021; Zeng et al., 2021). This method can effectively analyze the force, displacement and velocity of materials in the machine, and explore the movement process of particle swarm, which provides a theoretical basis for the structural design and parameter optimization of related machinery. It is necessary to establish a more accurate particle discrete element model before analyzing particle motion process by discrete element method (Chen et al., 2018; Zhou et al., 2020), and determine the basic physical parameters (density, Poisson's ratio, shear modulus) and contact mechanical parameters (collision recovery coefficient, static friction coefficient, rolling friction coefficient) (Zhao et al., 2022).

When the surface adhesion of materials is small, the model established based on Hertz-Mindlin (no slip) can be regarded as a whole in EDEM, which can carry out simulation analysis and optimization design for the conveying, grading, seeding and other processes of materials (Velický and Caroli, 2002; Hao et al., 2019; Xie et al., 2022). Nowadays, many scholars have completed the discrete element analysis and simulation of various materials. Shi et al. completed the establishment of flexible modulus of discrete element of flax stalk and the test verification of contact parameters Shi et al., 2023, Wang et al., 2016, Fang et al., 2022 used particle trajectory tracking to collect and calibrate parameters of corn straw; Zhang T. et al., 2020 established the corn straw discrete element model and verified its mechanical property parameters, which improved the accuracy of the discrete element method in the simulation of the corn straw crushing process; Li et al. (Li et al., 2022) established a discrete element model of corncob and calibrated its parameters. Park et al., 2021 created three particle models by applying the deviation based on the actual measurement size to analyze garlic cloves in DEM. By comparing AOR with the number of residual particles, and according to the simulation of the heap formation of garlic clove particles with various friction coefficients, they obtained the real simulation results of garlic clove particle contact parameters. Geng et al., 2021 calibrated the contact parameters of Oat without shell and Oat with shell by using discrete element method and graphic image processing techniques. In addition, parameters of wheat (Liu et al., 2016; Horabik et al., 2020; Sun et al., 2022), rice (Han et al., 2017; Zhang S. et al., 2020), soil (Zhou et al., 2014; Song et al., 2022), water chestnut (Zhang G. et al., 2022), oats and Vicia sativa mixed seed (Liao et al., 2022) were also calibrated.

In the field of discrete element simulation technology for agricultural materials, most of the research objects are grains such as maize, rice, and wheat. There are few detailed reports on the geometry of Zanthoxylum bungeanum granules, the establishment of discrete element models, and the acquisition of contact parameters. To simulate the picking process of Zanthoxylum bungeanum, it is necessary to conduct experiments to calibrate the relevant parameters. Compared with grains such as maize, rice, and wheat, Zanthoxylum bungeanum granules have significant differences in terms of their quality and shape. As a result, many related experiments are needed to explore the unique characteristics of their movement. By conducting these experiments, researchers can gain a deeper understanding of the behavior of Zanthoxylum bungeanum granules and establish accurate models for simulating their behavior during different processes.

In this paper, Zanthoxylum bungeanum granules were taken as the research object, and their intrinsic parameters and basic contact parameters were obtained by physical tests; The simulation model of Zanthoxylum bungeanum granules was established based on the bonding model, and the contact parameters of discrete element granules were calibrated. Finally, the calibration results of the parameters were verified by the test results of the angle of repose of Zanthoxylum bungeanum granules. The ultimate purpose of this article is to provide a model reference for the design and optimization of Zanthoxylum bungeanum picking machines. The workflow diagram is shown in Figure 1.

2 Materials and methods

2.1 Shape and size analysis of Zanthoxylum bungeanum granules

Hanyuan County in Ya'an City, Sichuan Province is known for producing Sichuan Hanyuan Zanthoxylum bungeanum. This variety of Zanthoxylum bungeanum has a long history and was even listed as a tribute during the Tang Dynasty, hence its nickname "tribute pepper" (Hou et al., 2022). Today, Sichuan Hanyuan Zanthoxylum bungeanum is popular both domestically and internationally due to its appealing red color, large and oily grains, rich aroma, and mellow and refreshing taste. It has become the most representative type of Zanthoxylum bungeanum. Therefore, the researchers chose to study Hanyuan tribute pepper in this research.

The actual particle shape and size of Zanthoxylum bungeanum are illustrated in Figure 2. Based on the morphology of Zanthoxylum bungeanum particles, the three mutually perpendicular axial dimensions, namely, length (L), width (W), and thickness (T), were defined as the characteristic dimensions. To account for individual variability, this study randomly selected and measured overall dimensions of 100 Zanthoxylum bungeanum granules sold in the market, using an electronic vernier caliper. The average length, width, and thickness were statistically determined to be 5.512, 4.999, and 4.892 mm, respectively.

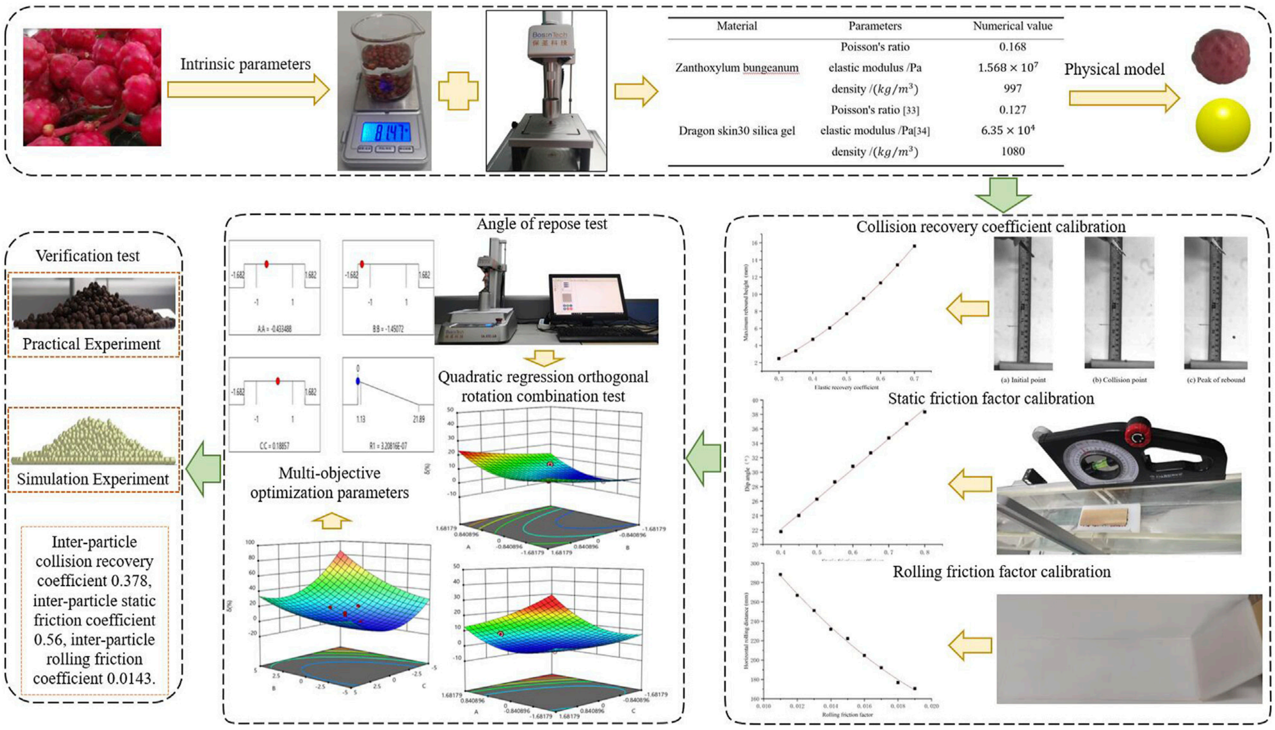

FIGURE 1
Flowchart of main steps of discrete element model calibration of Zanthoxylum bungeanum granules.

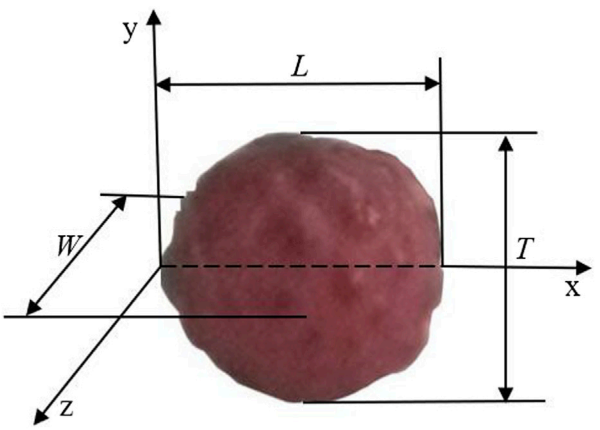

FIGURE 2
Shape and Size of the Zanthoxylum bungeanum granules.

2.2 Intrinsic parameters

The intrinsic parameters include density, Poisson's ratio and elastic modulus. Where density ρ measured by immersion method, the calculation formula (Gao et al., 2017) is

$$\rho = \frac{m\rho_1}{m_1 - m_2} \tag{1}$$

Where ρ_1 is the density of water, g/cm^3; m is the mass of Zanthoxylum bungeanum granules, g; m_1 is the mass of water and Zanthoxylum bungeanum granules, g; m_2 is the mass of water, g.

To weigh the Zanthoxylum bungeanum granules and water accurately, a high-precision electronic scale with an accuracy of 0.01 g was utilized. To minimize any reading errors, 20 Zanthoxylum bungeanum granules were grouped together, while 200 granules were randomly divided into 10 groups. The resulting density measurement for Zanthoxylum bungeanum granules was determined to be $0.997 g/cm^3$.

Poisson's ratio μ is defined as the ratio of transverse deformation to axial deformation of Zanthoxylum bungeanum granules under uniaxial tension or compression. It is an elastic index that reflects the transverse deformation characteristics of Zanthoxylum bungeanum granules. The calculation formula for Poisson's ratio (Zhang G. et al., 2022) is:

$$\mu = \left|\frac{\delta_1}{\delta_2}\right| = \frac{W_1 - W_2}{L_1 - L_2} \tag{2}$$

Where δ_1 is the lateral deformation of Zanthoxylum bungeanum, mm; δ_2 is the axial deformation of Zanthoxylum bungeanum, mm; W_1、 W_2 are the transverse dimensions of Zanthoxylum bungeanum before and after compression, mm; L_1、 L_2 are the axial dimensions of Zanthoxylum bungeanum before and after compression, mm.

The elastic modulus E represents the ability of Zanthoxylum bungeanum granules to resist elastic deformation during compression testing. The calculation formula for the elastic modulus (Zhang G. et al., 2022) is

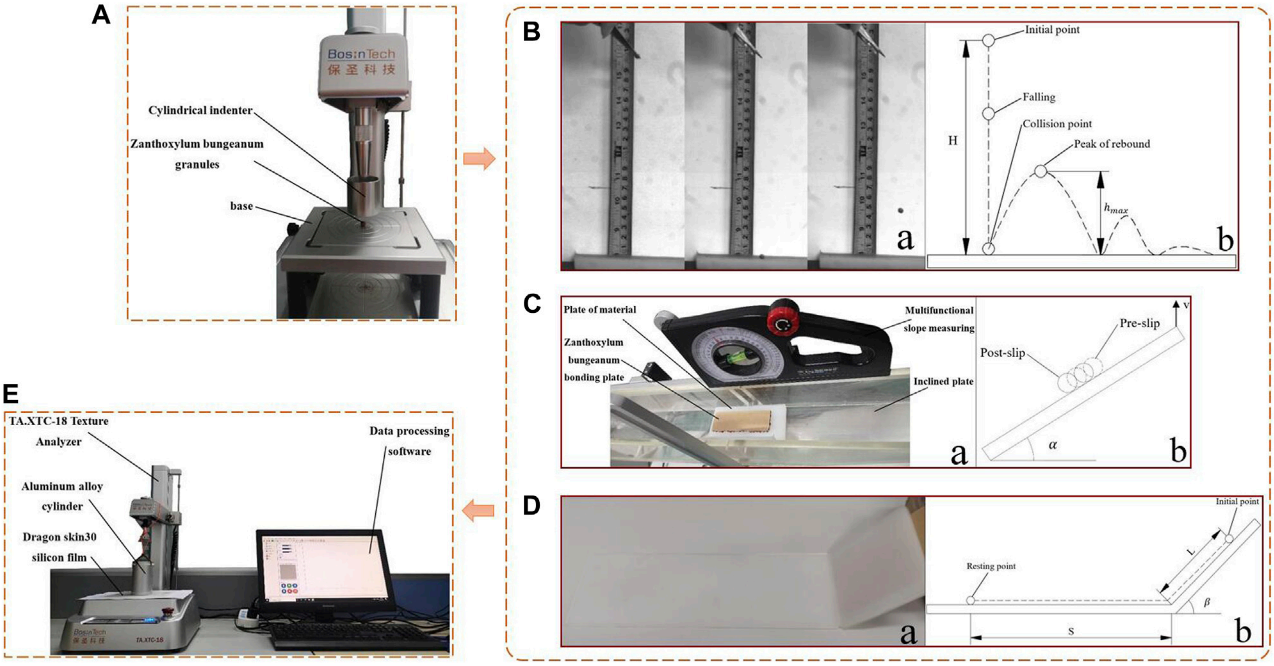

FIGURE 3
Flow chart of physical test for parameter calibration of discrete element model of Zanthoxylum bungeanum granules. **(A)** Uniaxial compression test; **(B)** Elastic recovery test, where a is the bench test diagram, b is the test flow diagram; **(C)** Test device for inclined plane slip test, where a is the bench test diagram, b is the test flow diagram; **(D)** Rolling friction factor test, where a is the bench test diagram, b is the test flow diagram; **(E)** Determination of Angle of repose of Zanthoxylum bungeanum granules.

$$E = \frac{F \cdot L}{S \cdot \Delta L} \tag{3}$$

Where, F is the maximum bearing capacity of Zanthoxylum bungeanum in elastic deformation stage, N; L is the initial length of the sample, mm; S is the cross-sectional area of the sample, mm^2 ; ΔL is the length difference before and after sample compression, mm.

Due to their small size and irregular shape, Zanthoxylum bungeanum granules cannot be cut into regular cubes. Instead, they are slightly flattened in the transverse direction with slightly elongated ends. To accurately measure the dimensions of the granules, a digital vernier caliper can be used to measure the major axis (L) and minor axis (W) of the ellipse, as shown in Figure 2.

The stressed sectional area of Zanthoxylum bungeanum, i.e., the effective area S, is calculated as (Liu et al., 2010)

$$S = \frac{3}{4} \times \frac{L}{2} \times \frac{W}{2}\pi \tag{4}$$

In this study, the Poisson's ratio and elastic modulus of Zanthoxylum bungeanum granules were determined through uniaxial compression testing using a TA. XTC-18 texture analyzer, as shown in Figure 3A. A flat indenter was selected at the end of the texture analyzer, and the granules were loaded at a rate of 5 mm/min (Hao et al., 2021). The test was repeated 20 times, and the resulting Poisson's ratio for the Zanthoxylum bungeanum sample was found to be 0.168, while the elastic modulus was 15.68 MPa.

3 Establishment of discrete element model of Zanthoxylum bungeanum granules

3.1 Physical model of Zanthoxylum bungeanum granules

To establish a discrete element model of Zanthoxylum bungeanum granules, EDEM simulation software was utilized. The sphericity ratio (Ye et al., 2023) was used to calculate the granule shape, and the formula used for this calculation is:

$$\varphi = \frac{\sqrt[3]{LWT}}{L} \times 100\% \tag{5}$$

Where, L is the length of Zanthoxylum bungeanum granules, mm; W is the width of Zanthoxylum bungeanum granules, mm; T is the thickness of Zanthoxylum bungeanum granules, mm. Based on the calculated sphericity rate of 93.02%, the Zanthoxylum bungeanum granules were modeled as single round particles using EDEM simulation software, as shown in Figure 1. For contact modeling during simulation tests, the Hertz Mindlin (no slip) contact mechanics model was selected to simulate the contact behavior of the granules, due to the small adhesion of the particle surfaces (Velický and Caroli, 2002).

TABLE 1 Simulation experiment parameters.

Material	Parameters	Numerical value
Zanthoxylum bungeanum	Poisson's ratio	0.168
	elastic modulus/Pa	1.568×10^7
	density/ (kg/m^3)	997
Dragon skin30 silica gel	Poisson's ratio	0.127
	elastic modulus/Pa	6.35×10^4
	density/ (kg/m^3)	1080

3.2 Simulation test parameters

The Dragon Skin 30 silica gel was used as the contact material in this research device. Table 1 presents the characteristic parameters of both the Zanthoxylum bungeanum granules and the contact material (Rus and Tolley, 2015; Xie and Li, 2021).

4 Contact parameter calibration

4.1 Calibration of contact parameters between Zanthoxylum bungeanum granules and materials

4.1.1 Elastic recovery coefficient calibration

The coefficient of restitution of Zanthoxylum bungeanum was determined by free fall test. In this paper, FASTCAM Mini UX100 high-speed camera is selected to collect the jumping height of pepper particles, and Photron FASTCAM Viewer software is used to view and scale the jumping height of seeds, as shown in Figure 3B. To obtain the clearest images, the high-speed camera was set to a frame rate of 500 fps after debugging. To minimize the influence of wind on the test results, a windless room was selected as the testing site. A Dragon Skin 30 silicone sheet was placed horizontally, and Zanthoxylum bungeanum granules were randomly selected, clamped with tweezers, and placed at a height of H = 40 mm above the material plate. At the start of the test, the tweezers were released, allowing the granules to bounce against the material plate. The maximum rebound height h_{max} was then measured using a high-speed camera system. This process was repeated five times, and the mean and standard deviation were calculated. The Photron FASTCAM Viewer software was used to analyze the rebound process of the Zanthoxylum bungeanum granules and obtain the maximum rebound height, which was determined by reading the ruler value. The elastic recovery coefficient is the ratio of the normal relative separation velocity v_1 and the normal relative approach velocity v_2 of the contact points of two objects before and after the collision, which can be expressed as the ratio of the maximum rebound height h_{max} and the initial fall height H in the collision between the seed and the material plate. The calculation formula (Liao et al., 2022) is

$$\mathbf{e} = \frac{\mathbf{v_1}}{\mathbf{v_2}} = \sqrt{\frac{\mathbf{h_{max}}}{\mathbf{H}}} \tag{6}$$

Based on the experimental results, it was determined that the Zanthoxylum bungeanum granules rebounded up to a maximum height of 6 mm on the Dragon Skin 30 silicone sheet. The average rebound height was calculated to be $\bar{h}$ = 4.69 mm, with a standard deviation of s = 0.862, which indicated relatively stable data. Therefore, the coefficient of restitution for the collision of the Zanthoxylum bungeanum granules was calculated as e = 0.548.

To avoid interference, all contact parameters other than the collision restitution coefficient between particles and materials were set to 0 in the EDEM simulation test. After the pre-simulation test, a range of the collision restitution coefficient between the Zanthoxylum bungeanum granules and the material plate was set to 0.3–0.7 with a set interval of 0.5. In the simulation test, the particles were initially generated at a height of 40 mm above the material plate, and then released with an initial velocity of 0. The acceleration was set to the gravitational acceleration to simulate the process of free fall. The mean value was computed over five repeated tests for each group. The simulation results for the collision restitution coefficient are presented in Table 2.

The simulation test results presented in Table 2 were plotted as a scatter plot using Origin 2018 software and fitted to obtain a fitting curve, as shown in Figure 4A. The fitting equation between the collision restitution coefficient and the maximum rebound height h_{max} between the Zanthoxylum bungeanum granules and Dragon Skin 30 silica gel sheets is given by:

$$\mathbf{h_{max} = 33.34e^2 - 0.26e - 0.52\left(R^2 = 0.999\right)} \tag{7}$$

The fitting results demonstrated that the maximum rebound height of the Zanthoxylum bungeanum granules increased with an increase in the collision restitution coefficient between the granules and materials, which is consistent with the findings of Liao et al. (Liao et al., 2022) and Guo et al. (Guo et al., 2022). This is because a higher collision restitution coefficient implies stronger deformation recovery ability and greater elastic potential energy of the granules during collision. According to the Law of Conservation of Momentum, the potential energy is converted into kinetic energy, resulting in a higher rebound speed and rebound height of Zanthoxylum bungeanum granules. The determination coefficient R^2 of the fitting equation is close to 1, indicating high reliability of the fitting equation. By substituting the maximum rebound height measured during the actual test into Equation 7, the elastic recovery coefficient was calculated to be e = 0.437. The simulation test was carried out using this value of the elastic recovery coefficient, and the mean value was obtained from five repetitions. The maximum rebound height was found to be 5.746 mm, with a relative error of 4.23% when compared to the measured value. These results demonstrate good consistency between the simulation test and the actual test results after calibration. Therefore, the elastic recovery coefficient between the Zanthoxylum bungeanum granules and Dragon Skin 30 silica gel sheets is determined to be 0.437.

4.1.2 Static friction coefficient calibration

The static friction coefficient μ_m between the Zanthoxylum bungeanum granules and the material plate was measured using an inclined plane slip test, as shown in Figure 3C. The test was performed on a theoretical mechanics multifunctional testing bench.

TABLE 2 Elastic recovery coefficient between Zanthoxylum bungeanum granules and Dragon skin30 silicone tablets.

Serial number	Elastic recovery coefficient	Maximum rebound height of Zanthoxylum bungeanum granules (h_{max}/mm)
1	0.3	2.477
2	0.35	3.391
3	0.4	4.72
4	0.45	6.058
5	0.5	7.707
6	0.55	9.503
7	0.6	11.317
8	0.65	13.42
9	0.7	15.605

The material plate was attached to the tilting plate, which was initially placed horizontally. To prevent particle rolling and reduce test errors, the Zanthoxylum bungeanum granules were attached to a rectangular board and placed on one end of the material plate. The incline plate was then slowly raised at a uniform rate until the Zanthoxylum bungeanum bonding plate began to slide. The incline plate was fixed, and the incline angle α was measured and recorded using a multifunctional slope measuring instrument. The experiment was repeated five times, and the average value was calculated. The Dragon Skin 30 silicone sheet was inclined at an angle of 37.04°.

In the EDEM simulation test, the calibrated elastic restitution coefficient is set. After the preliminary experiment, the range of static friction coefficient is set between 0.4 and 0.8 with an interval of 0.05. Other contact parameters are set to 0. In the simulation test, the Zanthoxylum bungeanum bonding plate was first generated on the material plate, and then one end of the material plate was lifted at a speed of 0.01 m/s until the Zanthoxylum bungeanum bonding plate slid. Each test was repeated five times to obtain the average value. The simulation test results of the collision restitution coefficient are shown in Table 3.

The relationship between tilt Angle and static friction coefficient was obtained through Table 3, and the test results were fitted with curves through Origin 2018 software. The simulation test results were drawn into scatter plot and fitted, and the fitting curve was obtained, as shown in Figure 4B. The fitting equation of static friction coefficient

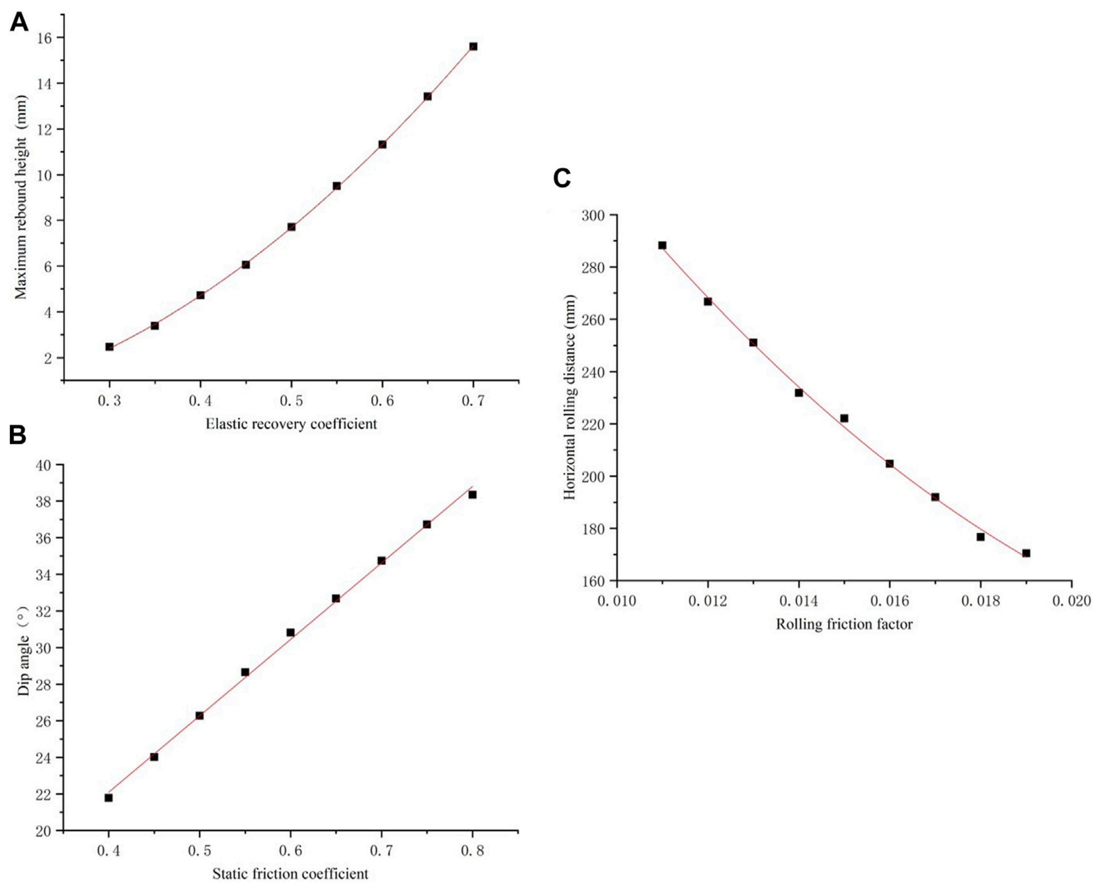

FIGURE 4
The fitting curve of contact parameters simulation test between Zanthoxylum anthoxylum granules and material. **(A)** Fitting curve of elastic recovery coefficient and maximum bounce height; **(B)** Fitting curve of static friction coefficient and dip angle; **(C)** Fitting curve of rolling friction factor and horizontal rolling distance.

TABLE 3 Static friction coefficient between Zanthoxylum bungeanum and Dragon skin30 silicone tablets.

Serial number	Static friction coefficient μ_m	Dip angle (α/°)
1	0.4	21.78
2	0.45	24.012
3	0.5	26.28
4	0.55	28.656
5	0.6	30.816
6	0.65	32.67
7	0.7	34.74
8	0.75	36.72
9	0.8	38.34

μ_m and inclination Angle α between Zanthoxylum bungeanum granules and Dragon skin30 silicone tablets is

$$\alpha = 41.766\mu_m + 5.386\left(R^2 = 0.997\right) \quad (8)$$

The fitting curve shows that the slip angle of the Zanthoxylum bungeanum bonding plate increases with an increase in the static friction coefficient, which is consistent with the trend obtained by Zhang S. et al. (2022). The determination coefficient of the fitting equation (R^2 = 0.997) indicates that the fitting equation has high reliability. By substituting the inclination angle of the inclined plane measured during the actual test into Equation 8, the static friction coefficient μ_m was calculated to be 0.758. The simulation was repeated five times to obtain the average value. The results show that the inclination angle of the inclined plane is 36.72°, with a relative error of 0.864% when compared to the measured value. These findings indicate that the calibrated simulation test results are consistent with the actual test results. Therefore, the static friction coefficient between the Zanthoxylum bungeanum granules and Dragon Skin 30 silicon sheets is determined to be μ_m = 0.758.

4.1.3 Rolling friction factor calibration

The rolling friction factor μ_n, between the particle and the material plate was measured by the inclined plane rolling method, as shown in Figure 3D. Due to the non-ideal spherical shape of the granules, large values of the inclination angle β and the rolling distance L can cause bouncing during the rolling process, which can adversely affect the accuracy of the test results. Conversely, for small values of β and L, the rolling distance of the particles is small, which is not conducive to precise measurements. Therefore, after conducting several pre-test adjustments, the inclination angle β was set to 45° and the rolling distance L of the slope was set as 40 mm. For the test, the granules were released with an initial velocity of 0 and allowed to roll down the inclined plane. The horizontal rolling distance S of the particles was measured after they reached the horizontal plane. The test was repeated five times on prickly ash particles, and the average value was taken. The horizontal rolling distance of Zanthoxylum bungeanum granules on Dragon Skin 30 silicone sheets was found to be 241.3 mm.

In the EDEM simulation test, the calibrated elastic recovery coefficient and static friction coefficient are respectively set by the same method. The range of rolling friction factor is set to 0.011–0.019, step size is set to 0.001, and other contact parameters are set to 0. For the simulation test, the setting was identical to that of the physical test. The slope angle was 45°, the particles were generated 40 mm away from the horizontal plane of the slope with no initial velocity release, and the particles were allowed to roll along the slope. The horizontal rolling distance of the particles at rest was then measured. Each group of tests was repeated 5 times to take the average value. The simulation test results of dynamic friction coefficient were shown in Table 4.

The simulation test results in Table 4 were plotted as a scatter diagram and fitted using Origin 2018 software. The fitting curve obtained is shown in Figure 4C, and the equation for the relationship between the rolling friction factor and horizontal rolling distance (S) between Zanthoxylum bungeanum and Dragon Skin 30 silicone sheets is

$$S = 584110.389\mu_n^2 - 32293.665\mu_n + 571.729\left(R^2 = 0.996\right) \quad (9)$$

Assuming that the granule is an ideal sphere and only affected by rolling friction in the pure rolling process, it can be obtained by the law of conservation of energy

$$mgL\sin\beta = mg\left(L\cos\beta + S\right)\mu_n \quad (10)$$

According to Equation 10, the horizontal rolling distance is inversely proportional to the rolling friction factor, assuming that the particle mass, tilt angle, and rolling distance of the inclined plane are all unchanged. This is consistent with the trend observed in the fitted curve obtained from the experimental results, and is similar to the results discussed by Zhang et al. (Zhang K. et al., 2022). The determination coefficient R^2 of the fitting equation is close to 1, indicating high reliability. Substituting the horizontal rolling distance S = 241.3 mm of Zanthoxylum bungeanum particles measured in the actual test into Equation 9, we obtain a rolling friction factor of μ_n = 0.0136. The average horizontal rolling distance of five simulation tests was 242.006 mm. The relatively small 2.927% relative error between the calibrated simulation test results and the actual test results indicates that the determined values are in good agreement. Therefore, the rolling friction factor between Zanthoxylum bungeanum granules and Dragon Skin 30 silicone sheets was determined to be μ_n = 0.0136.

4.2 Calibration of contact parameters between Zanthoxylum bungeanum granules

In this paper, the experimental results of Zanthoxylum bungeanum granule density and Angle of repose are compared with the simulation results, and the feasibility of the proposed zanthoxylum chinensis particle pile modeling method is preliminarily verified. In the process of Zanthoxylum bungeanum picking, Zanthoxylum bungeanum granules will squeeze each other under the pressure of fingers and palms, which has a significant impact on the accuracy of the discrete element model of contact parameters between Zanthoxylum bungeanum granules. Angle of repose refers to the Angle between the conical base line and the bottom surface accumulated when the bulk

TABLE 4 Rolling friction factor between Zanthoxylum bungeanum and Dragon skin30 silicone tablets.

Serial number	Rolling friction factor μ_n	Horizontal rolling distance (S/mm)
1	0.011	288.215
2	0.012	266.678
3	0.013	251.092
4	0.014	231.848
5	0.015	222.093
6	0.016	204.72
7	0.017	191.952
8	0.018	176.694
9	0.019	170.499

material falls naturally and continuously to a flat surface from a certain height. It can reflect the internal friction and scattering characteristics of the bulk material and is affected by the shape, material size and moisture content (Wang et al., 2022). In the experiment, with the relative error between the measured value and the simulated value of the angle of repose of Zanthoxylum bungeanum granules as the test index, and the interspecific contact parameter of Zanthoxylum bungeanum granules as the test factor, the steepest climbing test and the three factors quadratic regression orthogonal rotation combination design experiment were conducted. The simulation contact parameters of Zanthoxylum bungeanum granules were determined by optimizing the test results.

4.2.1 Angle of repose test

In this paper, the method of bottomless cylinder is used to test the angle of repose. The inner diameter and height of bottomless cylinder made of aluminum alloy are 60 mm and 100 mm respectively, and the cylinder is pasted with Dragon skin30 silica gel sheet. For testing, the bottom of the cylinder is in contact with the square Dragon skin30 silicon film with a side length of 180 mm, and Zanthoxylum bungeanum granules are filled with the cylinder, as shown in Figure 3E. Lift the cylinder vertically at the speed of 0.5 mm/s through TA. XTC-18 texture analyzer, and the particles slowly flow out from the bottom of the cylinder to form a cone. When the slope surface of the particle pile is stable, a camera was used to catch the front view of the particle resting angle, and repeat the test for five times.

In order to reduce the error in measuring the angle of repose of Zanthoxylum bungeanum granules, Matlab was used to process the edge image of the particle pile collected after the test. The image was denoised, gray-scaled, and binarized to obtain the boundary curve of the pile, which was then fitted with a line. The slope of the fitted line represents the tangent value of the particle stacking angle. Five repeated tests were performed in each group, and the average value was calculated to obtain the measured angle of repose of Zanthoxylum bungeanum granules, which was found to be 17.559°.

4.2.2 Steepest climb test

Just like the contact parameters between Zanthoxylum bungeanum granules and materials, the contact parameters between Zanthoxylum bungeanum granules have a significant impact on the simulation of the picking process. Therefore, it is important to measure and calibrate the collision recovery coefficient, static friction coefficient, and rolling friction coefficient between Zanthoxylum bungeanum granules. The preliminary test results indicate that the collision recovery coefficient ranges from 0.1 to 0.8, the static friction coefficient ranges from 0.41 to 0.90, and the rolling friction coefficient ranges from 0.011 to 0.018. The steepest climb test was used to determine the zero level and optimal value interval of the quadratic regression orthogonal rotation combination test factors. The test scheme and results of the steepest climb test are shown in Table 5. This experiment enables the authors to optimize the simulation parameters and obtain an accurate representation of the behavior of Zanthoxylum bungeanum granules during the picking process.

From Table 5, it can be observed that the error between the simulated angle of repose and the measured angle of repose is the smallest for the fourth group of combination tests. Therefore, it can be concluded that the actual contact parameters are most likely to be close to the values used in the fourth group of combination. Based on this, the authors selected groups 3, 4 and 5 as the coded values for the three factors quadratic regression orthogonal rotation combination test.

4.2.3 Quadratic regression orthogonal rotation combination test

Based on the results of steepest climb test, taking the elastic recovery coefficient, static friction coefficient and rolling friction factor between Zanthoxylum bungeanum granules as the test factors, and the relative error between the Angle of repose of the simulation test and the Angle of repose of the bench test as the test index, a three factors quadratic regression orthogonal rotation combination test was conducted. The coding of the simulation test factors is shown in Table 6. The design scheme and results of the simulation test are shown in Table 7. A, B and C are the factor coding values.

Design-Expert software was used to perform multiple regression fitting on the test data, and the significance test of the regression equation was shown in Table 8. According to Table 8, the regression model is extremely significant, but the loss of fit is not significant, indicating that the regression equation fits well. The quadratic regression equation fitted by the model is consistent with the practice, and can correctly reflect the relationship between Angle of repose θ and test factors A, B and C, which is similar to the conclusion obtained by Shi et al. (14). Inter-particle elastic recovery coefficient, inter-particle static friction coefficient and inter-particle rolling friction factor have extremely significant effects on Angle of repose error. After data processing, response surfaces were obtained, as shown in Figure 5. As can be seen from the figure, the relative error of the Angle of repose first decreases and then increases with the inter-particle elastic recovery coefficient, increases with the increase of the inter-particle static friction coefficient, and decreases with the increase of the inter-particle rolling friction factor. AB, AC and BC have no significant influence on the error of the Angle of repose, which may be because the three factors have significant influence on the error of the Angle of repose.

After removing the insignificant term from the regression equation, the new regression equation obtained by fitting is

TABLE 5 Test scheme and results of steepest climb test.

Serial number	Inter-particle collision recovery coefficient e_x	Inter-particle coefficient of static friction $\boldsymbol{\mu}_x$	Inter-particle coefficient of rolling friction $\boldsymbol{\mu}_y$	Simulation angle of repose θ/°	Relative error δ/%
1	0.1	0.41	0.011	16.155	7.99%
2	0.2	0.48	0.012	16.630	5.29%
3	0.3	0.55	0.013	17.134	2.42%
4	0.4	0.62	0.014	17.749	1.08%
5	0.5	0.69	0.015	17.947	2.21%
6	0.6	0.76	0.016	18.383	4.7%
7	0.7	0.83	0.017	19.091	8.72%
8	0.8	0.9	0.018	20.009	13.95%

TABLE 6 Factor coding of simulation test.

Code	Test factors		
	e_x	$\boldsymbol{\mu}_x$	$\boldsymbol{\mu}_y$
−1.682	0.3	0.55	0.013
−1	0.35	0.585	0.0135
0	0.4	0.62	0.014
1	0.45	0.655	0.0145
1.682	0.5	0.69	0.015

$$\boldsymbol{\delta = 5.9 + 4.05A + 3.63B - 3.04C + 3.06A^2 \left(R^2 = 0.92\right)} \tag{11}$$

The *p*-value of the regression model is less than 0.01, indicating that the regression equation model is very significant. Moreover, the *p*-value of the missing fitting term is much larger than 0.05, indicating that the non-normal error takes a small proportion in the fitting of the regression Equation 11 and the actual, and there are no other major factors affecting the index. The determination coefficient $R^2 = 0.92$ of the regression equation indicates that the regression equation has a high degree of fitting, and can accurately reflect the relationship between the experimental factors and the relative error of the Angle of repose, which can be used to predict the Angle of repose.

4.2.4 Multi-objective optimization parameters

Using the optimization module of Design Expert software, aiming at the minimum relative error of Angle of repose, the regression equation was solved, the response surface was analyzed, and the regression model was optimized.

$$\begin{cases} \text{target value} = \mathbf{17.559^\circ} \\ \text{s.t.} \begin{cases} \mathbf{0.3 \le A \le 0.5} \\ \mathbf{0.55 \le B \le 0.69} \\ \mathbf{0.013 \le C \le 0.015} \end{cases} \end{cases} \tag{12}$$

The optimization results of central combination parameters are shown in Figure 6. The optimal parameter combination of the regression model is as follows: inter-particle elastic recovery coefficient 0.378, inter-particle static friction coefficient 0.56, and inter-particle rolling friction factor 0.0143.

TABLE 7 Test scheme and results.

Serial number	Test factors			Relative error δ/%
	A	B	C	
1	−1	−1	−1	3.06%
2	1	−1	−1	13.52%
3	−1	1	−1	9.73%
4	−1	−1	1	21.89%
5	1	1	−1	1.34%
6	−1	−1	1	7.89%
7	1	−1	1	8.18%
8	1	1	1	12.56%
9	−1.682	0	0	8.96%
10	1.682	0	0	21.89%
11	0	−1.682	0	1.13%
12	0	1.682	0	14.78%
13	0	0	−1.682	16.59%
14	0	0	1.682	2.77%
15	0	0	0	5.61%
16	0	0	0	10.42%
17	0	0	0	6.24%
18	0	0	0	2.45%
19	0	0	0	4.48%

4.3 Verification test

After optimizing the contact parameters using the three-factors quadratic regression orthogonal rotation combination test, the

10.3389/fmech.2023.1204659

TABLE 8 Analysis of variance.

Source	Sum of squares	df	Mean square	F-value	*p*-value
Model	680.19	9	75.58	11.83	0.0005**
A-A	223.89	1	223.89	35.03	0.0002**
B-B	179.46	1	179.46	28.08	0.0005**
C-C	125.94	1	125.94	19.71	0.0016**
AB	0.0276	1	0.0276	0.0043	0.949
AC	17.08	1	17.08	2.67	0.1365
BC	1.56	1	1.56	0.2437	0.6333
A2	127.44	1	127.44	19.94	0.0016**
B2	2.35	1	2.35	0.367	0.5596
C2	14.32	1	14.32	2.24	0.1686
Residual	57.52	9	6.39	—	—
Lack of Fit	22.98	5	4.6	0.5325	0.7475
Pure Error	34.53	4	8.63	—	—
Cor Total	737.71	18	—	—	—

Note: * indicates significant impact ($p \leq 0.05$), * * indicates extremely significant impact ($p \leq 0.01$).

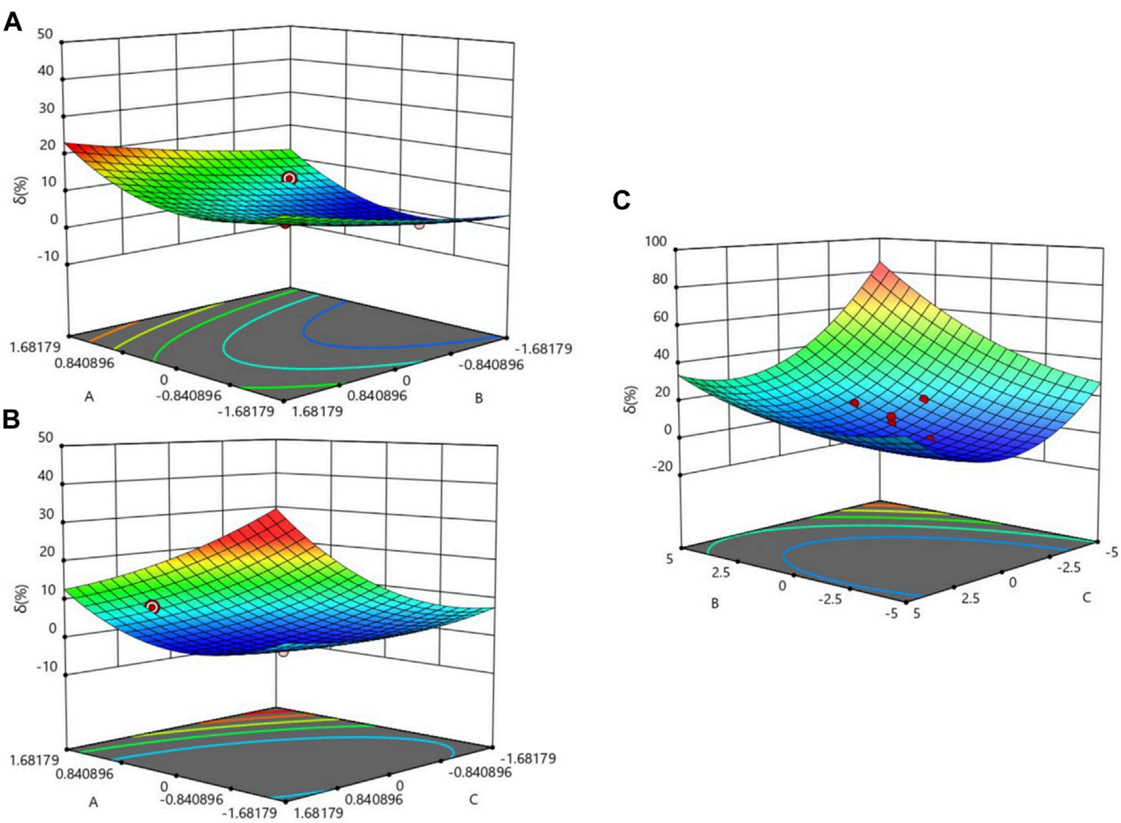

FIGURE 5
Response Surface. **(A)** Effect of test factors A and B on response surface of angle of repose; **(B)** Effect of test factors A and C on response surface of angle of repose; **(C)** Effect of test factors B and C on response surface of angle of repose.

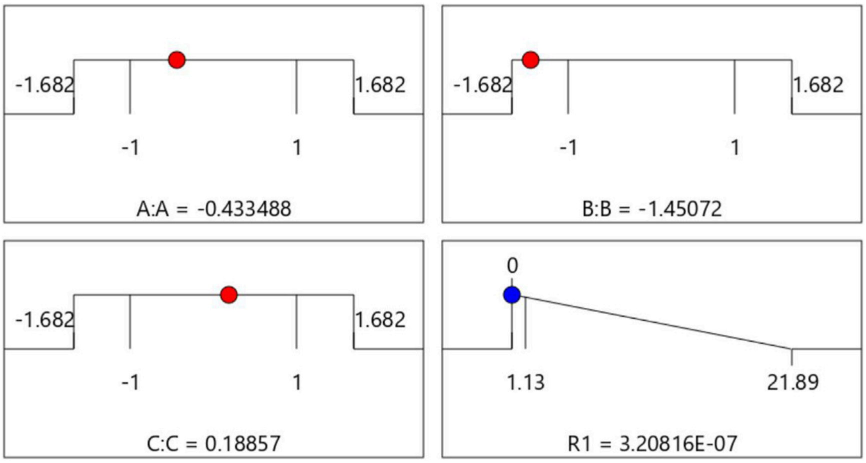

FIGURE 6
Optimization results of central combination parameters.

FIGURE 7
Shape comparison between practical experiment and simulation experiment. **(A)** Practical experiment; **(B)** Simulation experiment.

authors substituted the values into EDEM software to conduct five simulation tests of the angle of repose. The results of the simulation tests showed an average measured angle of repose of 17.523°, with a relative error of only 0.204% between the measured angle of repose and the bench test. The comparison between the test results and the simulation results is shown in Figure 7. The small error between the actual value of the accumulation test and the simulation value indicates that there is no significant difference between them. This verifies the accuracy of the simulation test, and these results can be used in discrete element correlation simulation experiments related to Zanthoxylum bungeanum.

5 Discussion

This paper proposed a method for calibrating parameters of Zanthoxylum bungeanum granules. The simulation parameters are calibrated according to the macroscopic parameters obtained from the physical test of Angle of repose. This method can also be used for parameter calibration of other complex models. The main conclusions of this paper are summarized as follows.

1) Taking Zanthoxylum bungeanum granules as the research object, the basic physical parameters (density, Poisson's ratio, elastic modulus) of discrete element simulation of Zanthoxylum bungeanum granules were determined by physical test method, and the discrete element model of Zanthoxylum bungeanum granules was established in EDEM software by Hertz-Mindlin (no slip) model.
2) By using the combination of bench test and simulation test, the elastic recovery coefficient, static friction coefficient and rolling friction factor between Zanthoxylum bungeanum granules and Dragon skin 30 silica gel sheets were calibrated through impact test, inclined sliding test and inclined rolling test. The elastic recovery coefficient between Zanthoxylum bungeanum granules and Dragon skin30 silica gel sheet is 0.437, the static friction coefficient is 0.758, and the rolling friction factor is 0.0136.
3) The actual Angle of repose of mixed seeds was 17.559° through the accumulation test of Zanthoxylum bungeanum granules.

With the coefficient of interspecific elastic recovery, interspecific static friction and interspecific rolling friction as experimental factors, and with the relative errors of the actual accumulation Angle and the simulated value of EDEM as experimental indexes, a three-factor quadratic regression orthogonal rotation combination test was carried out. The mathematical models of factors and indicators are established. The optimum values of contact parameters are as follows: inter-particle elastic recovery coefficient 0.378, inter-particle static friction coefficient 0.56, inter-particle rolling friction factor 0.0143.

4) In order to verify the reliability of parameter calibration results, the Angle of repose physical test was conducted. The relative error between the simulated test value and the theoretical value is 0.204%, which verifies the feasibility and effectiveness of the proposed modeling method.

Data availability statement

The raw data supporting the conclusions of this article will be made available by the authors, without undue reservation.

Author contributions

Conceptualization, LC and JW; methodology, JW and YT; software, JW, ZC and QW; validation, LC, YT and QW; formal analysis, LC and ZC; investigation, YT; resources, LC, YT and ZC; data curation, JW and QW; writing—original draft preparation, JW; writing—review and editing, JW, LC and YT; project administration, LC and DH; funding acquisition, DH. All authors contributed to the article and approved the submitted version.

Funding

This research was funded by Science and Technology Innovation and Entrepreneurship Seedling Project in Ya'an City, Sichuan Province, China.

Acknowledgments

We thank Sichuan Agricultural University for providing us with the working facilities.

Conflict of interest

The authors declare that the research was conducted in the absence of any commercial or financial relationships that could be construed as a potential conflict of interest.

Publisher's note

All claims expressed in this article are solely those of the authors and do not necessarily represent those of their affiliated organizations, or those of the publisher, the editors and the reviewers. Any product that may be evaluated in this article, or claim that may be made by its manufacturer, is not guaranteed or endorsed by the publisher.

References

Chen, Z., Yu, J., Xue, D., Wang, Y., Zhang, Q., and Ren, L. (2018). An approach to and validation of maize-seed-assembly modelling based on the discrete element method. *Powder Technol.* 328, 167–183. doi:10.1016/j.powtec.2017.12.007

Fang, M., Yu, Z., Zhang, W., Cao, J., and Liu, W. (2022). DEM parameter acquisition and calibration of corn stalk non-spherical particles using particle trajectory tracking. *Granul. Matter* 24, 110–111. doi:10.1007/s10035-022-01269-9

Fang, M., Yu, Z., Zhang, W., Liu, W., Bie, Z., and Song, J. (2021). Analysis and test on the motion process of grinding Material of Disc Cutter type hay Cutter. *Trans. Chin. Soc. Agric. Eng.* 37, 76–84.

Fu, R. (2011). Current situation and development trend of orchard picking machinery. *Agric. Dev. Equip.* 2011, 17–19.

Gao, Y., Si, Z., Wang, L., Zhang, X., Chang, J., and Qiao, H. (2017). Preventive and therapeutic effect of brozopine on stroke in Dahl Salt-sensitive hypertensive rats. *Guangzhou Chem. Ind.* 45 (20), 137–147. doi:10.1016/j.brainres.2017.07.019

Geng, L., Zuo, J., Lu, F., Jin, X., Sun, C., and Ji, J. J. (2021). Calibration and experimental validation of contact parameters for oat seeds for discrete element method simulations. *Appl. Eng. Agric.* 37, 605–614. doi:10.13031/aea.14381

Guo, S., Wan, P., Yang, J., Deng, Z., Wang, S., Zhu, M., et al. (2022). Discrete element based calibration and test of simulation parameters for fish feed. *J. Huazhong Agric. Univ.* 41 (06), 286–295.

Han, Y., Jia, F., Zeng, Y., Jiang, L., Zhang, Y., and Cao, B. (2017). DEM study of particle conveying in a feed screw section of vertical rice mill. *Powder Technol.* 311, 213–225. doi:10.1016/j.powtec.2017.01.058

Hao, J., Long, S., Li, H., Jia, Y., Ma, Z., and Zhao, J. (2019). Discrete element model construction and simulation parameter calibration of machine-harvested Yam. *Trans. Chin. Soc. Agric. Eng.* 35, 34–42.

Hao, J., Wei, W., Huang, P., Qin, J., and Zhao, J. (2021). Discrete element parameter calibration and experimental verification of oil sunflower kernel. *Trans. Chin. Soc. Agric. Eng.* 37, 36–44.

Horabik, J., Wiącek, J., Parafiniuk, P., Bańda, M., Kobyłka, R., Stasiak, M., et al. (2020). Calibration of dis-crete-element-method model parameters of bulk wheat for storage. *Biosyst. Eng.* 200, 298–314. doi:10.1016/j.biosystemseng.2020.10.010

Hou, W., Lian, T., and Peng, X. (2022). Multiple measures to promote the flourishing development of county characteristic agricultural products - taking Hanyuan prickly Ash as an example. *Rural. Revital.* 2022, 54–55.

Li, R., Wu, Y., Li, S., Han, D., Yang, L., Yang, M., et al. (2021). Simulation analysis and parameter optimization of vibrating Prickly ash picker based on ANSYS Workbench and ADAMS. *J. Southwest Univ. Nat. Sci. Ed.* 43, 57–67. doi:10.1016/j.strueco.2021.01.008

Li, X., Du, Y., Liu, L., Zhang, Y., and Guo, D. (2022). Parameter calibration of corncob based on DEM. *Adv. Powder Technol.* 33, 103699. doi:10.1016/j.apt.2022.103699

Liao, Y., You, Y., Wang, D., Zhang, X., Zhang, H., and Ma, W. (2022). Parameters calibration and experiment on discrete element model of oats and Vicia sativa mixed seeds. *Trans. Chin. Soc. Agric. Mach.* 53, 14–22.

Liu, F., Zhang, J., Li, B., and Chen, J. (2016). Calibration of parameters of wheat required in discrete element method simulation based on repose angle of particle heap. *Trans. Chin. Soc. Agric. Eng.* 32, 247–253.

Liu, Z., Wen, J., Bleich, D., Salgame, P., and Gause, W. C. (2010). Regulation of type 1 diabetes, tuberculosis, and asthma by parasites. *Grain storage* 39, 27–38. doi:10.1007/s00109-009-0546-0

Liu, Z., Zhao, X., Yang, L., Li, J. Y., Hou, B., Hu, J. M., et al. (2017). Triterpenoids and iridoids from Patrinia scabiosaefolia. *Mach. Build. Automation* 46, 130–135. doi:10.1016/j.fitote.2017.04.011

Lu, Y., Yi, W., Xiong, C., Tuo, H., and Wang, P. (2020). Present situation and development trend of hand-held prickly ash picking ma-chinery. *Agric. Technol. Inf.* 2020, 69–73. doi:10.15979/j.cnki.cn62-1057/s.2020.22.027

Park, D., Lee, C. G., Yang, D., Kim, D., Kim, J. Y., and Rhee, J. Y. (2021). Analysis of inter-particle contact parameters of garlic cloves using discrete element method. *J. Biosyst. Eng.* 46, 332–345. doi:10.1007/s42853-021-00110-0

Rus, D., and Tolley, M. T. J. N. (2015). Design, fabrication and control of soft robots. *Nature* 521, 467–475. doi:10.1038/nature14543

Shi, R., Dai, F., Zhao, W., Zhang, F., Shi, R., and Guo, J. (2023). Establishment of discrete element flexible modulus of flax stem and verification of contact parameters. *Trans. Chin. Soc. Agric. Mach.* 2023, 1–11.

Song, Z., Li, H., Yan, Y., Tian, F., Li, Y., and Li, F. (2022). Parameter calibration and experiment of discrete element simulation model of soil non-equidiameter particles in Mulberry Garden. *Trans. Chin. Soc. Agric. Mach.* 53, 21–33.

Sun, K., Yu, J., Liang, L., Wang, Y., Yan, D., Zhou, L., et al. (2022). A DEM-based general modelling method and experimental verification for wheat seeds. *Powder Technol.* 401, 117353. doi:10.1016/j.powtec.2022.117353

Velický, B., and Caroli, C. J. P. R. E. (2002). Pressure dependence of the sound velocity in a two-dimensional lattice of Hertz-Mindlin balls: Mean-field description. *Mean-field Descr.* 65, 021307. doi:10.1103/physreve.65.021307

Wang, J., Zhao, S., Gao, L., Yuan, Y., and Yang, Y. (2021). Design and experiment of passive disc stubble Cutter with self-adjusting cutting Angle in corn ridge cropping. *Trans. Chin. Soc. Agric. Mach.* 52, 59–67.

Wang, S., Yu, Z., Aorigeleand Zhang, W. (2022). Study on the modeling method of sunflower seed particles based on the discrete element method. *Comput. Electron. Agric.* 198, 107012. doi:10.1016/j.compag.2022.107012

Wang, Y., Liang, Z., Zhang, D., Cui, T., Shi, S., Li, K., et al. (2016). Calibration method of contact characteristic parameters for corn seeds based on. *EDEM* 32, 36–42.

Xie, D., Zhang, C., Wu, X., Wang, W., Liu, L., and Chen, L. (2022). Design and experiment of garlic seed drainer assisted by air suction with disturbing seed teeth. *Trans. Chin. Soc. Agric. Mach.* 53, 47–57.

Xie, Y., and Li, H. (2021). Simulation study on the clamping performance of soft pneumatic gripper made of Silica gel. *J. Zhejiang Sci-Tech Univ. Nat. Sci. Ed.* 45, 328–334.

Ye, D., Zhao, J., Qing, J., Shen, B., Weng, H., and Zheng, S. (2023). Design and test of key components of small electric helical fertilizer. *J. Shenyang Agric. Univ.* 54 (01), 81–89.

Zeng, w., Ma, X., Cao, X., Li, Z., and Wang, X. (2021). Application status and prospect of discrete element method in agricultural en-gineering research. Transactions of the Chinese Society for Agricultural Machinery. *Trans. Chin. Soc. Agric. Mach.* 52, 1–20.

Zhang, G., Chen, L., Liu, H., Dong, Z., Zhang, Q., and Zhou, Y. (2022). Discrete element simulation parameter calibration and experi-ment of Water chestnut. *Trans. Chin. Soc. Agric. Eng.* 38, 41–50.

Zhang, K., Hou, C., Sun, B., Su, Z., and Liu, T. J. (2022). Extracellular vesicles from human hepatic progenitor cells accelerate deep frostbite wound healing by promoting fibroblasts proliferation and inhibiting apoptosis. *Agric. Res. Arid Areas.* 40 (06), 286–293. doi:10.1016/j.jtv.2021.10.009

Zhang, S., Zhang, R., Chen, T., Fu, J., and Yuan, H. (2022). Calibration of simulation parameters of mung bean seeds using discrete element method and verification of seed-metering test. *Trans. Chin. Soc. Agric. Mach.* 53 (03), 71–79.

Zhang, S., Tekeste, M. Z., Li, Y., Gaul, A., Zhu, D., and Liao, J. (2020). Scaled-up rice grain modelling for DEM calibration and the vali-dation of hopper flow. *Biosyst. Eng.* 194, 196–212. doi:10.1016/j.biosystemseng.2020.03.018

Zhang, T., Zhao, M., Liu, F., Tian, H., Wulan, T., Yue, Y., et al. (2020). A discrete element method model of corn stalk and its mechanical characteristic parameters. *BioResources* 15, 9337–9350. doi:10.15376/biores.15.4.9337-9350

Zhao, L., Zhou, H., Xu, L., Song, S., Zhang, C., and Yu, Q. (2022). Parameter calibration of coconut bran substrate simulation model based on discrete element and response surface methodology. *Powder Technol.* 395, 183–194. doi:10.1016/j.powtec.2021.09.065

Zhou, H., Chen, Y., and Sadek, M. A. (2014). Modelling of soil–seed contact using the Discrete Element Method (DEM). *Biosyst. Eng.* 121, 56–66. doi:10.1016/j.biosystemseng.2014.02.006

Zhou, L., Yu, J., Wang, Y., Yan, D., and Yu, Y. (2020). A study on the modelling method of maize-seed particles based on the discrete element method. *Powder Technol.* 374, 353–376. doi:10.1016/j.powtec.2020.07.051